SLM and PTS Peak-Power Reduction of OFDM Signals Without Side Information

A. D. S. Jayalath, *Member, IEEE*, and C. Tellambura, *Senior Member, IEEE*

***Abstract*—Selected mapping (SLM) and partial transmit sequence (PTS) are well-known techniques for peak-power reduction in orthogonal frequency-division multiplexing (OFDM). We derive a simplified maximum likelihood (ML) decoder for SLM and PTS that operates without side information. This decoder exploits the fact that the modulation symbols belong to a given constellation and that the multiple signals generated by the PTS or SLM processes are widely different in a Hamming distance sense. Pairwise error probability (PEP) analysis suggests how SLM and PTS vectors should be chosen. The decoder performs well over additive white Gaussian noise (AWGN) channels, fading channels, and amplifier nonlinearities.**

***Index Terms*—Orthogonal frequency-division multiplexing (OFDM), partial transmit sequences, peak-to-average power ratio, selected mapping.**

I. Introduction

ORTHOGONAL frequency-division multiplexing (OFDM) has been standardized in many wireless applications with high-speed data transmission due to many advantages that it offers in fading channels [1]. However, the OFDM signal consists of a large number of independently modulated subcarriers, which can yield a large peak-to-average power ratio (PAR) when the subcarriers add up coherently. A large PAR leads to disadvantages such as increased complexity of the analog-to-digital converter and a reduced efficiency of the radio frequency amplifier. Many solutions to the PAR problem have recently been proposed [2]–[7].

Partial transmit sequences (PTSs) and selected mapping (SLM) reduce the PAR by generating $U > 1$ statistically independent OFDM symbols for a given data frame and transmitting the $\tilde{u}$th symbol with the lowest peak power [8]. The value of $\tilde{u}$ (side information) is required to recover the signal successfully. Clearly, $\log_2(U)$ bits are required to represent this information, which is of critical importance to the receiver. One solution is to reserve several subcarriers (i.e., pilot tones) for side information. In a frequency-selective fading channel, such pilot tones may be lost and an irrevocable decoding error can occur. Extra protection bits may need to be sent and the total redundancy can thus exceed $\log_2(U)$ bits.

Consequently, recent research has modified the original SLM concept to make it operate without side information. Breiling *et al.* propose a scrambling scheme that does not use explicit side information [9]. A multimode coding technique based on guided scrambling is proposed in [10]. Modified repeat accumulate codes are used to generate statistically independent symbols in [11]. Although the techniques in [9]–[11] do not use explicit side information, a small amount of redundancy is introduced at the transmitter. Standard arrays of linear block codes are proposed in [12], and this technique sacrifices the error-correcting ability of the channel code for recovering side information at the receiver.

In this letter, we develop a new decoder for SLM and PTS without side information. The key idea is to exploit the fact that the set of the U symbols have large Hamming distances and therefore contain inherent diversity that can be exploited at the receiver. We therefore derive the maximum likelihood (ML) decoder for SLM and, using optimum hard decision for each subcarrier, obtain the new decoder with drastically reduced complexity. The performance loss of the simplified ML decoder over the ML decoder is negligible.

For coded orthogonal frequency-division multiplexing (COFDM), the receiver can use minimum-distance decoding via the Viterbi algorithm. As linear block codes, convolutional codes, and trellis codes have well-defined trellises, our receiver can be integrated into the channel decoder itself. For uncoded OFDM, it is prohibitive to search all possible sequences, and we thus derive a suboptimal metric. We compare our decoder against an idealized receiver that has perfect side information. We show that the performance degradation is negligible for two particularly important cases: 1) a nonlinear amplifier is applied to OFDM signals with SLM; and 2) subcarriers experience Rayleigh fading. Moreover, for AWGN channels, our decoder shows a performance virtually identical with the ideal receiver.

II. PAR of Orthogonal Frequency-Division Multiplexing

An OFDM symbol is formed by a block of N modulation symbols and N orthogonal subcarriers, such that the adjacent subcarrier separation $\Delta f = 1/T$ and T is the OFDM signal duration. The resulting signal may be expressed as

$$s(t) = \frac{1}{\sqrt{N}} \sum_{n=0}^{N-1} c_n \mathrm{e}^{j2\pi n \Delta f t}, \quad 0 \le t \le T. \tag{1}$$

Manuscript received August 29, 2003; revised March 7, 2004 and July 6, 2004; accepted October 31, 2004. The editor coordinating the review of this paper and approving it for publication is T. M. Duman. Dr. Jayalath is funded by the National ICT Australia (NICTA). NICTA is funded by the Australian Department of Communications, Information and Technology and the Arts and the Australian Research Council through "Backing Australia's Ability" and the ICT Centre of Excellence Program.

A. D. S. Jayalath is with the Department of Information Engineering, Research School of Information Sciences and Engineering, Australian National University, Canberra A.C.T. 0200, Australia and also with National ICT Australia Limited, Canberra A.C.T. 2601, Australia (e-mail: Dhammika.Jayalath@anu.edu.au).

C. Tellambura is with the Department of Electrical and Computer Engineering, University of Alberta Edmonton, AB T6G 2V4, Canada (e-mail: chintha@ece.ualberta.ca).

Digital Object Identifier 10.1109/TWC.2005.853916

The subcarrier vector in (1), $\mathbf{c} \in \mathcal{C}$, $\mathbf{c} = (c_0, c_1, \ldots, c_{N-1})$ is a vector of N constellation symbols from a constellation $\mathcal{Q}$. The size of $\mathcal{Q}$ is q. For COFDM, $\mathcal{C}$ is an optional channel code such as a convolutional code or a trellis code. A cyclic prefix (CP) is added to the signal $s(t)$ in order to avoid the intersymbol interference (ISI) that occurs in multipath channels. Since the CP does not impact the PAR issue, we ignore it. The PAR of OFDM is given by

$$\xi = \frac{\max |s(t)|^2}{E\left\{|s(t)|^2\right\}} \tag{2}$$

where $E\{.\}$ denotes expectation. PAR does not greatly depend on the constellation $\mathcal{Q}$. The theoretical maximum of the PAR for N number of subcarriers is $10\log(N)$ dB.

III. Selected Mapping Without Side Information

The SLM encoder uses U vectors (SLM vectors) given by

$$\mathbf{P}_u = \left[\mathrm{e}^{j\phi_0^u}, \mathrm{e}^{j\phi_1^u}, \ldots, \mathrm{e}^{j\phi_{N-1}^u}\right]$$

where $\phi_n^u \in (0, 2\pi]$ and $u \in \{0, 1, \ldots, U-1\}$. Let $\mathbf{a} \otimes \mathbf{b}$ represent the vector product of $\mathbf{a}$ and $\mathbf{b}$. For a given input frame $\mathbf{c}$, the lowest PAR sequence $\mathbf{c} \otimes \mathbf{P}_{\tilde{u}}$, $\tilde{u} \in \{0, 1, \ldots, U-1\}$, is selected for transmission. In the subsequent development, the value of the optimal transmit sequence number $\tilde{u}$ is "NOT" transmitted to the receiver.

We derive the new decoder using the following properties. 1) c_n's are restricted to a given signal constellation $\mathcal{Q}$. 2) The set of $\mathbf{P}_u$'s is fixed and known *a priori*. 3) $\mathbf{c} \otimes \mathbf{P}_u$ and $\mathbf{c} \otimes \mathbf{P}_v$ are sufficiently different for $u \neq v$. The necessary condition for this method to work is $c_n \mathrm{e}^{j\phi_n^u} \notin \mathcal{Q}$ for all n and u. The set of $\mathbf{P}_u$ can be chosen readily to ensure this. We expect the performance of the decoder to be very good, as the Hamming distance between any $\mathbf{P}_u$ and $\mathbf{P}_v$ is very large. For simplicity, let us assume a distortionless and noiseless channel. Now, the receiver gets $\mathbf{r} = \mathbf{c} \otimes \mathbf{P}_{\tilde{u}}$ and computes $\mathbf{r} \otimes \mathbf{P}_u^*$ for $u = 0, \ldots, U-1$. Note that $\mathbf{r} \otimes \mathbf{P}_u^*$ will not be a vector of symbols from the constellation $\mathcal{Q}$ unless $u = \tilde{u}$. This observation allows us to dramatically reduce the complexity of the ML decoder.

Consider the received signal r_n after the FFT demodulation at the receiver

$$r_n = H_n c_n \mathrm{e}^{j\phi_n^{\tilde{u}}} + n_n \tag{3}$$

where H_n is the frequency response of the fading channel at the nth subcarrier and n_n is a complex additive white Gaussian noise (AWGN) sample. The signal-to-noise ratio (SNR) is defined as $\gamma_s = E\{|H_n c_n|^2\}/E\{|\eta_n|^2\}$ where $E\{\}$ is the statistical expectation operator. Let $\mathbf{r} = [r_0, r_1, \ldots, r_{N-1}]$ and $\mathbf{H} = [H_0, H_1, \ldots, H_{N-1}]$. Without side information (not knowing $\tilde{u}$) the optimal ML decoder uses the decision metric

$$\mathcal{D} = \min_{\substack{[\hat{c}_0, \hat{c}_1, \ldots, \hat{c}_{N-1}] \in \mathcal{C} \\ \mathbf{P}_{\hat{u}}, \hat{u} \in \{0,1,\ldots,U-1\}}} \sum_{n=0}^{N-1} \left| r_n \mathrm{e}^{-j\phi_n^{\hat{u}}} - H_n \hat{c}_n \right|^2. \tag{4}$$

This minimization can be performed as follows. The minimum distance $\mathbf{H} \otimes \hat{\mathbf{c}}$ to $\mathbf{r} \otimes \mathbf{P}_0^*$ is determined, where $\mathbf{P}_0^*$ is the conjugate of $\mathbf{P}_0$. This can be done by the Viterbi algorithm for coded systems or by searching all q^N data sequences for uncoded q-ary modulation. This process is repeated for $\mathbf{P}_1, \mathbf{P}_2, \ldots, \mathbf{P}_{U-1}$. The global minimum distance solution yields the best estimates for $\mathbf{c}$ and $\tilde{u}$. The overall complexity is U times that of COFDM without SLM.

Consider the quaternary phase-shift keying (QPSK) constellation given by

$$\mathcal{Q}_{\mathrm{QPSK}} = \left\{\mathrm{e}^{\frac{j\pi m}{2}}, m = 0, 1, \ldots, 3\right\}. \tag{5}$$

For the uncoded case, there are $U4^N$, $|.|^2$ operations to solve (4). This is of very high complexity and can be performed only for small N. Thus, a suboptimal decoding metric with reduced complexity is derived next.

Let r_n be detected into the nearest constellation point $\hat{c}_n$, by comparing r_n with $\hat{H}_n \hat{c}_n \mathrm{e}^{j\phi_n^{\hat{u}}}$, where $\hat{H}_n$ is the estimated channel response. That is, a hard decision is made for each subcarrier. This whole process is repeated for $0 \leq \hat{u} \leq U-1$. The minimum Euclidean distance solution yields the data sequence. The simplified new decision metric can thus be written as

$$\mathcal{D}_{\mathrm{SLM}} = \min_{\mathbf{P}_{\hat{u}}, \hat{u} \in \{0,1,\ldots,U-1\}} \sum_{n=0}^{N-1} \min_{\hat{c}_n \in \mathcal{Q}} \left| r_n \mathrm{e}^{-j\phi_n^{\hat{u}}} - \hat{H}_n \hat{c}_n \right|^2. \tag{6}$$

Fig. 1 depicts the proposed decoder structure. For COFDM with a given trellis structure, the metric (6) can be computed using the Viterbi algorithm. The branch metric of the trellis may be given by

$$\mathcal{B} = \left| r_n \mathrm{e}^{-j\phi_n^{\hat{u}}} - \hat{H}_n \hat{c}_n \right|^2. \tag{7}$$

Here, $\hat{c}_n$ is a branch label of the trellis. Initial results of this receiver have been presented in [13].

SLM vectors for the proposed system are constructed by selecting each ϕ_n^u randomly between 0 and 2π, subject to the constraint that $\mathrm{e}^{j\phi_n^u}$ is not a member of $\mathcal{Q}$.

IV. Partial Transmit Sequences

The input data vector $\mathbf{c}$ is partitioned into disjoint subblocks, as $\{\mathbf{c}_m | m = 0, 1, \ldots, M-1\}$, and these are combined to minimize the PAR. Phase angles of subcarriers in each subblock are changed, and several iterations are performed before obtaining the optimally combined sequence. The inverse discrete Fourier transform (IDFT) of the $\mathbf{c}_m$ are called PTSs. Let $y_{k,m}$ for $k = 0, 1, \ldots, LN-1$, $m = 0, 1, \ldots, M-1$, be the LN point IDFT of the $\mathbf{c}_m$ appropriately zero-padded

$$y_{k,m} = \sum_{n \in I_m} c_n \mathrm{e}^{\frac{j2\pi nk}{LN}} \tag{8}$$

where $I_m \in \{0, 1, \ldots, N-1\}$ is the subset of indices belonging to the mth subblock and L is the oversampling factor.

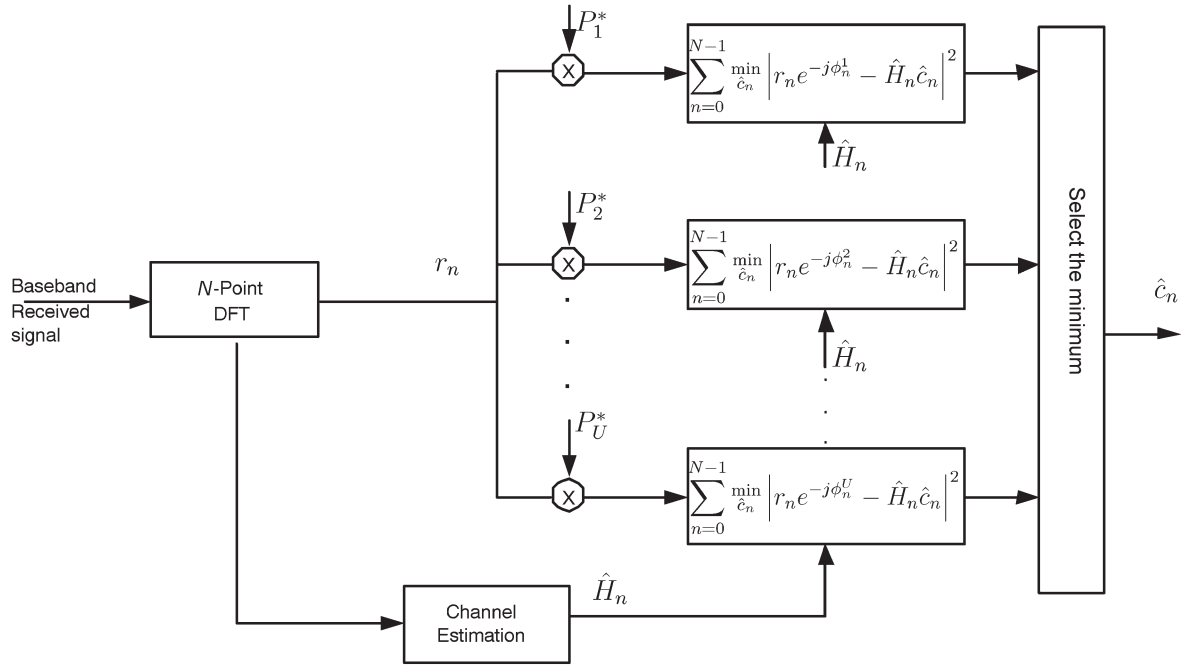

Fig. 1. Proposed decoder structure.

Using the linearity property of the IDFT, the time domain samples can be represented as

$$s_k = \sum_{m=1}^{M} b_m y_{k,m}, \quad k = 0, 1, \ldots, LN-1 \tag{9}$$

where $\{b_m,\ m = 0, 1, \ldots, M-1\}$ are weighting factors. They are further assumed to be pure rotations (i.e., $b_m = \mathrm{e}^{j\phi_m}$). The weighting factors are chosen to minimize $|s_k|$. Finally, the optimal PAR ($\xi_{\text{opt.}}$) can be found using

$$\xi_{\text{opt.}} = \min_{b_1,\ldots,b_M} \left(\max_{0 \le k \le LN} \left| \sum_{m=1}^{M} b_m y_{k,m} \right|^2 \right). \tag{10}$$

If the weighting factors ($\mathbf{b} = [\mathrm{e}^{j\phi_1}, \mathrm{e}^{j\phi_2}, \ldots \mathrm{e}^{j\phi_M}]$) are limited to v phases, (10) requires v^{M-1} iterations to obtain the optimal solution. Note that the above development is similar to [14] except for the use of oversampling.

For coherent demodulation, the optimized weighting factors $\hat{b}_m$ are required at the receiver. When $\hat{b}_m$ is a continuous value, an infinite number of bits will be required as side information. The solution to this problem is to select $\hat{b}_m$ from a finite set of quantized weighting factors. However, the proposed decoder allows us to select arbitrary values for the weighting factors as the receiver does not depend on the side information [15].

We now limit the weighting factors to a codebook, which is constructed as follows. Select a vector of $M-1$ weighting factors, which are equally distributed along the unit circle

$$\mathbf{v} = \left[\mathrm{e}^{j\left(\left(\frac{2\pi}{M-1}+\theta\right)\right)}, \mathrm{e}^{j\left(\left(2\frac{2\pi}{M-1}+\theta\right)\right)}, \ldots, \mathrm{e}^{j(2\pi+\theta)} \right]. \tag{11}$$

TABLE I
SYSTEM AND CHANNEL PARAMETERS USED FOR SIMULATIONS

Parameter	Value
Total number of subcarriers	256
Number of pilots	16
Modulation	QPSK
Data rate	25 Mbps
TCM parameters	8 states, 8-PSK
Maximum Doppler frequency	555 Hz
OFDM symbol duration	19.2 μs
Guard interval	0.8 μs
Number of paths of the channel	6
Maximum delay spread of the channel	500 ns
Carrier frequency	5 GHz

The phase offset θ $(0 < \theta < \pi/2)$ can be any value such that components of $\mathbf{v}$ do not belong to $\mathcal{Q}$. The codebook B will then consists of all $(M-1)!$ permutations of $\mathbf{v}$. The PTS transmitter may try all $\mathbf{b} = [1, \mathbf{v}]$, where $\mathbf{v} \in B$ to reduce PAR or the PAR optimization can be stopped as soon as the PAR drops below a given threshold [16]. The identity of the optimal weighting sequence $\tilde{\mathbf{v}}$ is "NOT" transmitted to the receiver.

A. Decoding PTS-OFDM Signals Without Side Information

Consider the received signal r_n after the FFT demodulation at the receiver is given by (3). However, the encoded data is now given by $c_n \mathrm{e}^{j\tilde{\phi}_m}$, where $\mathrm{e}^{j\tilde{\phi}_m}$ $(\tilde{b}_m \in \mathbf{v})$ is the optimized weighting factor used in the mth subblock. The objective is

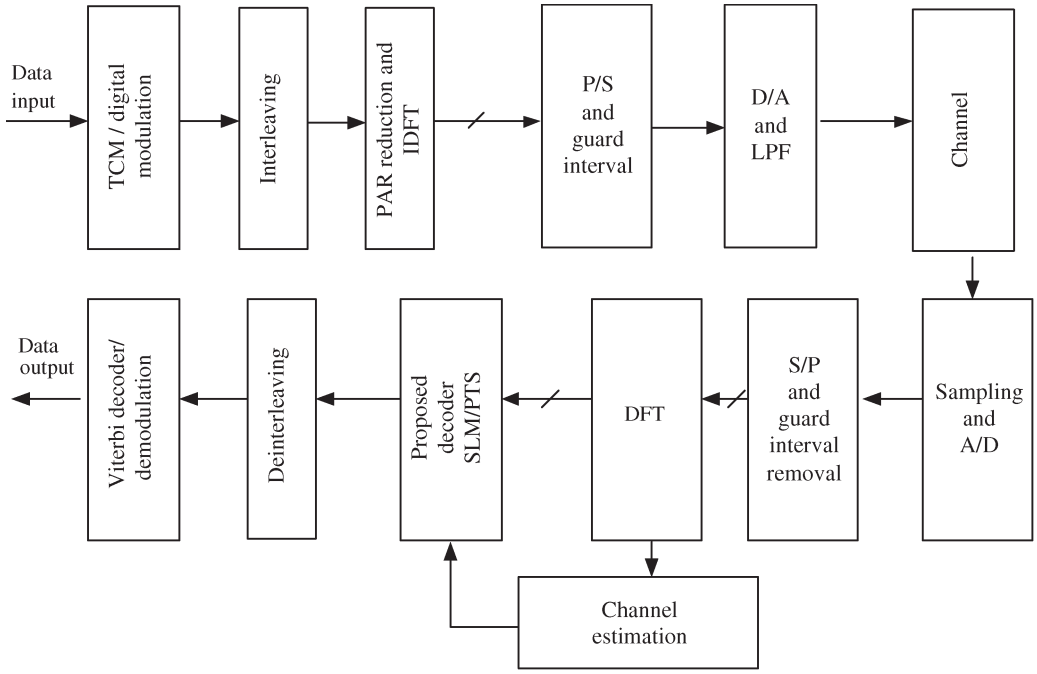

Fig. 2. System block diagram with channel interleaver and proposed decoder.

to determine the optimal weighting sequence $\tilde{\mathbf{v}}$. Letting $\mathbf{r} = [r_0, r_1, \ldots, r_{N-1}]$ and $\hat{\mathbf{H}} = [\hat{H}_0, \hat{H}_1, \ldots, \hat{H}_{N-1}]$, the decision metric used at the proposed PTS-OFDM decoder to determine the weighting factor of the mth subblock becomes

$$\mathcal{D}_{\mathrm{PTS}}^{m} = \min_{m\in\{0,1,\ldots,M-1\}} \sum_{n=\frac{Nm}{M}}^{\frac{N(m+1)}{M-1}} \min_{\hat{c}_n\in\mathcal{Q}} \left| r_n - \hat{H}_n \hat{c}_n \hat{b}_m \right|^2 \quad (12)$$

where $\hat{b}_m \in \mathbf{b}$ and $\hat{H}_n$ is the estimated channel. This metric can be evaluated as follows. For the nth subcarrier $(0 \le n \le N/M)$ of a subblock, the received symbol is detected into its nearest constellation point $\hat{c}_n$ by comparing r_n with value $\hat{H}_n^{-1} r_n \hat{b}_m^{-1}$. The Euclidean distance corresponding to this detection is stored. This process is repeated for all the subcarriers (N/M) in the mth subblock $0 \le n < N/M$. The minimum Euclidean distance solution is obtained by evaluating the metric for all weighting factors $(0 \le m \le M-1)$, which yields the correct weighting factor $(\tilde{b}_m)$ used for the mth subblock. Similarly, weighting factors for all the subblocks are determined. The proposed decoder does not rely on side information and can select the weighting factors without confining them to a set of quantized values.

V. Performance Analysis

The bit error rate (BER) performance of the decoder (4) is analyzed here. The decoder must decide both the transmitted sequence $\mathbf{c}$ and the SLM vector $\mathbf{P}_{\tilde{u}}$. The pairwise error probability (PEP) $P[(\mathbf{c}, \mathbf{P}_{\tilde{u}}) \to (\hat{\mathbf{c}}, \mathbf{P}_{\hat{u}})]$ is the probability of choosing $\hat{\mathbf{c}}$ and $\mathbf{P}_{\hat{u}}$ when indeed $\mathbf{c}$ and $\mathbf{P}_{\tilde{u}}$ were transmitted. We consider the case where $\hat{H}_n$ (an estimate of H_n) is known to the receiver and M-PSK signaling is used. The PEP is approximated using (13), which is defined at the bottom of the page (see Appendix). When the channel estimation (CE) SNR is high $(\gamma_e \longrightarrow \infty)$, (13) further simplifies to

$$P\left[(\mathbf{c}, \mathbf{P}_{\tilde{u}}) \to (\hat{\mathbf{c}}, \mathbf{P}_{\hat{u}})\right] \simeq \binom{2N-1}{N} \prod_{n=0}^{N-1} \frac{1}{\gamma_s \left| c_n e^{j\phi_n^{\tilde{u}}} - \hat{c}_n e^{j\phi_n^{\hat{u}}} \right|^2}. \quad (14)$$

This PEP expression is very insightful. Note that this clearly resembles the well-known asymptotic results of maximal ratio combining (MRC) of order N (see [20, pp. 14.4–18]). Therefore, this has an error equivalent of Nth order (MRC). This is called a diversity order. This explains that if an ML decoder is used, the error rate decrease as γ_s^{-N}. Note that without the SLM expansion process, the diversity order would be much

$$P\left[(\mathbf{c}, \mathbf{P}_{\tilde{u}}) \to (\hat{\mathbf{c}}, \mathbf{P}_{\hat{u}})\right] \simeq \binom{2N-1}{N} \prod_{n=0}^{N-1} \frac{\left[\frac{\gamma_s+\gamma_e-1}{\gamma_s(\gamma_e-1)}\right]^2}{\left\{\left(\frac{1}{\gamma_s} + \frac{1}{(\gamma_e-1)} + \left|c_n e^{j\phi_n^{\tilde{u}}} - \hat{c}_n e^{j\phi_n^{\hat{u}}}\right|^2\right)\left(\frac{1}{(\gamma_e-1)} + \frac{1}{\gamma_s}\right) - \left|\frac{1}{\gamma_s} + \frac{1}{\gamma_e}\hat{c}_n c_n^* e^{j(\phi_n^{\hat{u}} - \phi_n^{\tilde{u}})}\right|^2\right\}} \quad (13)$$

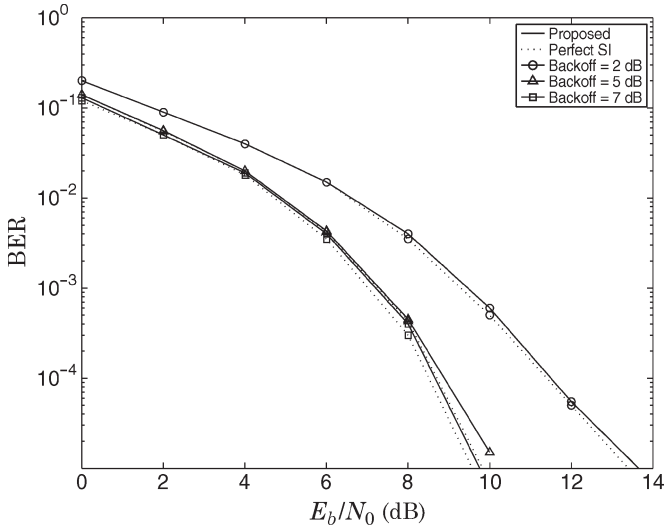

Fig. 3. Performance of the proposed SLM-OFDM decoder in AWGN channel and with a soft limiting nonlinear amplifier having backoff values of 2, 3, and 7 dB.

less than N. Since we choose ϕ_n^u uniform in $(0, 2\pi)$, the probability that $\phi_n^{\tilde{u}} = \phi_n^{\hat{u}}$ for $\tilde{u} \neq \hat{u}$ is zero. Note that if $\phi_n^{\tilde{u}}$ was chosen from a finite constellation such as QPSK, the achievable diversity order would be less than N. If SLM is "NOT" used at the transmitter, the numbers of n for which $c_n \neq \tilde{c}_n$ relate to the $d_{\min}$ (minimum Hamming distance) of the channel code (if used). If no channel code is used, $d_{\min} = 1$. The asymptotic error rate should then decrease as $\gamma_s^{-d_{\min}}$. We conclude that the use of long random phase sequence in SLM provides a diversity order of N. Since N is large, this ensures that our proposed decoders can achieve nearly ideal performance levels. Equation (14) also suggests the following decision rules for SLM code book generation.

1) For maximum diversity order, make sure that $\phi_n^k \neq \phi_n^l$ for all $l \neq k$.
2) Choosing ϕ_n^k from a uniform distribution ensures maximum diversity benefits.

VI. Simulation Results

Proposed decoders for both SLM and PTS are evaluated over AWGN and fading channels and in the presence of a nonlinear amplifier using Monte Carlo simulations. System and channel parameters are shown in Table I. The system block diagram for both uncoded and TCM-coded OFDM is shown in Fig. 2. The interleaver and deinterleaver pair is used for the simulation on frequency-selective fading channels to randomize the bit errors across subcarriers providing the frequency diversity.

Fig. 3 compares the performance of the proposed decoder (6) with an ideal SLM decoder using perfect side information (PSI-SLM) in AWGN. The two systems show virtually identical performance in AWGN. Comparative performance in AWGN for a soft limiter (nonlinearity) with backoff values of 2, 5, and 7 dB in Fig. 3 shows that both the decoders perform nearly identically.

Given the excellent decoder performance over AWGN and nonlinear channels, we next investigate its performance

TABLE II
Power Delay Profile of the Frequency-Selective Fading Channel

Index	Delay (ns)	Relative power (dB)
1	0	0
2	50	-4
3	100	-8
4	200	-16
5	300	-24
6	500	-39

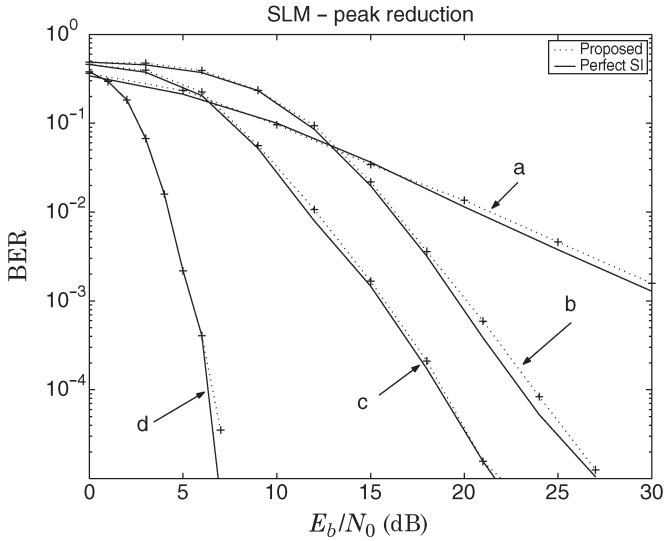

Fig. 4. BER of the several TC-OFDM systems with (a) uncoded OFDM with pilot-assisted CE, (b) TC-OFDM with pilot-assisted CE, (c) TC-OFDM with perfect CSI, and (d) TC-OFDM in an AWGN (no fading). Normalized Doppler frequency is 0.011.

for trellis-coded orthogonal frequency-division multiplexing (TC-OFDM) in frequency-selective fading channels. The frequency-selective channel model is given by $h(t) = \sum_{k=1}^{L} h_k \delta(t - kT)$ with $E[|h_k|^2]$ decaying exponentially with k (Table II). A normalized Doppler frequency of 0.011 is assumed in the simulations. We use a nonsystematic, eight-state encoder with eight-phase-shift keying (8-PSK) mapping, which has the same spectral efficiency as uncoded QPSK-OFDM. Each OFDM symbol consists of 64 pilot symbols for CE.

Fig. 4 shows that the proposed decoder has identical performance to a decoder with PSI in all the channels considered (a–d). Fig. 4 also shows the effect of imperfect channel state information (CSI). The proposed decoder performs well even with imperfect CSI and recovers COFDM completely in both AWGN and fading channels even in the presence of a nonlinear amplifier.

Fig. 5 compares the performance of the proposed decoder (12) with an ideal PTS receiver that has perfect side information (PSI-PTS) in AWGN and Rayleigh fading. As expected, the proposed decoder almost perfectly recovers the received data in AWGN. It performs nearly as good as the ideal receiver in Rayleigh fading. The slight performance degradation of the

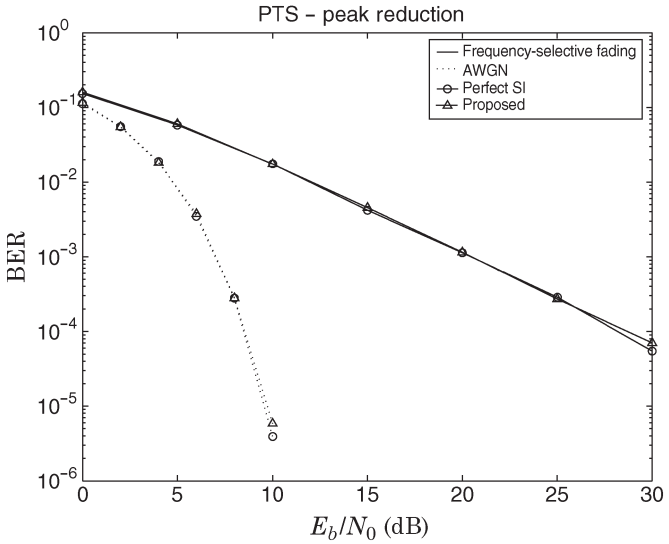

Fig. 5. Comparison of BER performance of the proposed decoder for PTS-OFDM in AWGN and fading with perfect CSI. Normalized Doppler frequency is 0.011.

proposed decoder in the fading channel may be overcome by a suitable channel coding scheme, as in the case of SLM.

The performance of the proposed decoder with higher order constellations (8-PSK and 16-QAM) was also simulated. In the high SNR region, the proposed decoder performs fairly close to the ideal case.

VII. Conclusion

Selected mapping (SLM) and partial transmit sequence (PTS) detection without using side information for coded orthogonal frequency-division multiplexing (COFDM) and orthogonal frequency-division multiplexing (OFDM) has been developed. These decoders recover received COFDM in additive white Gaussian noise (AWGN), fading, and the presence of nonlinear amplifiers. Analytical results show that the ML decoder for SLM has an Nth-order diversity effect in fading. As N is typically large, excellent performance can be obtained even though a suboptimal decoder (6) is used. The proposed SLM and PTS systems neither lose throughput due to side information nor degrade bit error rate (BER) due to errors in side information. However, a reduction in throughput occurs due to the pilot tones used for channel estimation (CE). Some increase in the receiver complexity is the price paid for these benefits.

Appendix
PEP Analysis

PEP analysis is a widely used approach for designing coding schemes such as trellis codes and space–time codes. This approach begins with the union bound for the BER. The union bound is a weighted sum of all the PEPs for a given code. As the SNR goes to infinity, the union bound is dominated by a handful of PEPs, which can be expressed in terms of distance properties of the code. In general, if the largest PEP decays as γ_s^{-d}, the coded system is said to have a diversity order of d. Note that this analysis is valid only in the high SNR regime. The interested reader is referred to [18] and [19]. We use this approach here to show that a side benefit of the SLM expansion process is to generate an equivalent system with a diversity order reaching N. We derive the PEP as a complex contour integral with distinct single-order poles. However, more insight can be gained by considering the high SNR regime where the multiple poles coalesce into an Nth-order pole. The resulting PEP expression is presented in Section V.

Let $\hat{H}_n = H_n + \epsilon_n$ where ϵ_n is a complex Gaussian noise affecting the CE process. We assume the estimation error ϵ_n to be independent of the channel additive noise and the channel. That is, $E[n_n\epsilon_m^*] = 0$ and $E[H_n\epsilon_m^*] = 0$. While this assumption may not be realistic in some cases, it greatly facilitates the subsequent analysis. Without loss of generality, we assume

$$E\left\{|H_n|^2\right\} = 1, \quad n = 0, 1, \ldots, N-1. \tag{15}$$

We define the CE SNR as

$$\gamma_e = \frac{E\left\{|\hat{H}_n|^2\right\}}{E\left\{|\epsilon_n|^2\right\}} \quad \text{for} \quad n = 0, 1, \ldots, N-1. \tag{16}$$

This means $E\{|\hat{H}_n|^2\} = \gamma_e/(\gamma_e - 1)$ and $E[|\epsilon_n|^2] = 1/(\gamma_e - 1)$. We also have $E\{H_n^*\hat{H}_n\} = E\{H_n^*(H_n + \epsilon_n)\} = 1$. We consider MPSK only for brevity.

From (3), we find $E\{|n_n|^2\} = 1/\gamma_s$ and $E\{|r_n|^2\} = 1 + (1/\gamma_s)$. The PEP is given by

$$P\left[(\mathbf{c}, \mathbf{P}_{\tilde{u}}) \to (\hat{\mathbf{c}}, \mathbf{P}_{\hat{u}})\right] = \Pr\left\{\sum_{n=0}^{N-1}\left|r_n - \hat{H}_n c_n e^{j\phi_n^{\tilde{u}}}\right|^2 > \sum_{n=0}^{N-1}\left|r_n - \hat{H}_n \hat{c}_n e^{j\phi_n^{\hat{u}}}\right|^2\right\}. \tag{17}$$

Let us consider a term

$$\begin{aligned} D_n &= \left|r_n - \hat{H}_n \hat{c}_n e^{j\phi_n^{\hat{u}}}\right|^2 - \left|r_n - \hat{H}_n c_n e^{j\phi_n^{\tilde{u}}}\right|^2 \\ &= |X_n|^2 - |Y_n|^2. \end{aligned} \tag{18}$$

This is a special case of the quadratic form, which has been analyzed by Proakis [20]. The complex Gaussian random variable X_n and Y_n are zero mean and correlated. We need their variances and the covariance for deriving the moment generating function (mgf) of D_n

$$\begin{aligned} \mu_{xx} &= \frac{1}{2}E\left\{|X_n|^2\right\} \\ &= \frac{1}{2}E\left\{|r_n|^2 + \left|\hat{H}_n \hat{c}_n e^{j\phi_n^{\hat{u}}}\right|^2 - 2\mathrm{Re}\left\{r_n^* \hat{H}_n \hat{c}_n e^{j\phi_n^{\hat{u}}}\right\}\right\} \\ &= \frac{1}{2}\left\{1 + \frac{1}{\gamma_s} + \frac{\gamma_e}{(\gamma_e - 1)} - 2\mathrm{Re}\left\{c_n^* \hat{c}_n e^{j\left(\phi_n^{\hat{u}} - \phi_n^{\tilde{u}}\right)}\right\}\right\}. \end{aligned} \tag{19}$$

For MPSK symbols, $|c_n - \hat{c}_n|^2 = 2 - 2\mathrm{Re}\{c_n \hat{c}_n^*\}$, therefore,

$$\mu_{xx} = \frac{1}{2}\left\{\frac{1}{\gamma_s} + \frac{1}{(\gamma_e - 1)} + \left|c_n e^{j\phi_n^{\tilde{u}}} - \hat{c}_n e^{j\phi_n^{\hat{u}}}\right|^2\right\}.$$

The variance of Y_n is given by

$$\begin{aligned}\mu_{yy} &= \frac{1}{2}E\left\{\left|-\epsilon_n c_n e^{j\phi_n^{\tilde{u}}} + n_n\right|^2\right\} \\ &= \frac{1}{2}\left\{\frac{1}{(\gamma_e - 1)} + \frac{1}{\gamma_s}\right\}.\end{aligned}$$

The covariance is given by

$$\begin{aligned}\mu_{xy} &= \frac{1}{2}E\left\{\left(r_n - \hat{H}_n \hat{c}_n e^{j\phi_n^{\hat{u}}}\right)\left(\epsilon_n^* c_n^* e^{j\phi_n^{\tilde{u}}} + n_n^*\right)\right\} \\ &= \frac{1}{2}\left\{\frac{1}{\gamma_s} + \frac{1}{(\gamma_e - 1)}\hat{c}_n c_n^* e^{j\left(\phi_n^{\hat{u}} - \phi_n^{\tilde{u}}\right)}\right\}. \qquad (20)\end{aligned}$$

In Proakis [20, eq. B-6], we use $\alpha_1 = \alpha_2 = 0$, $A = 1$, $B = -1$, and $C = 0$ and get

$$\omega_n = \frac{\mu_{xx} - \mu_{yy}}{4\left(\mu_{xx}\mu_{yy} - |\mu_{xy}|^2\right)} \qquad (21)$$

$$\begin{bmatrix} v_{1n} \\ v_{2n} \end{bmatrix} = \sqrt{\omega_n^2 + \frac{1}{4\left(\mu_{xx}\mu_{yy} - |\mu_{xy}|^2\right)}} \pm \omega_n. \qquad (22)$$

Note that for high SNR and high CE SNR (γ_e), we have $\mu_{xx} \geq \mu_{yy}$ and $\mu_{xy} \simeq 0$. In this case

$$\omega_n \simeq \frac{1}{4\mu_{yy}} = \frac{\gamma_s(\gamma_e - 1)}{2(\gamma_s + \gamma_e - 1)}.$$

The mgf of D_n is given by

$$\Phi_{D_n}(s) = E\{e^{sD_n}\} = \frac{v_{1n}v_{2n}}{(v_{1n} - s)(v_{2n} + s)}. \qquad (23)$$

To facilitate the analysis, we assume that the availability of perfect interleaving, making $D_n, n = 0, 1, \ldots, N-1$ independent. Consider a block interleaver of size $N_d \times N_s$. As a result of interleaving, the effective Doppler is increased by a factor of N_d (the interleaving depth) and this reduces temporal correlation. Perfect interleaving implies N_d being infinity. However, in practical cases, fairly small values of N_d are sufficient [21].

Assuming perfect interleaving, $D_n, n = 0, 1, \ldots, N-1$ are independent. The mgf of $D = \sum D_n$ is given by

$$\Phi_D(s) = \prod_{n=0}^{N-1} \frac{v_{1n}v_{2n}}{(v_{1n} - s)(v_{2n} + s)}. \qquad (24)$$

We assume that all $v_{1n} \neq v_{1m}$ for $m \neq n$ and $v_{2n} \neq v_{2m}$ for $m \neq n$. From (17), we find

$$P\left[(\mathbf{c}, \mathbf{P}_{\tilde{u}}) \to (\hat{\mathbf{c}}, \mathbf{P}_{\hat{u}})\right] = \Pr(D < 0). \qquad (25)$$

Using a complex variable theory, this can be written as

$$P\left[(\mathbf{c}, \mathbf{P}_{\tilde{u}}) \to (\hat{\mathbf{c}}, \mathbf{P}_{\hat{u}})\right] = -\mathrm{Res}\left\{\frac{\Phi_D(s)}{s} \text{ at poles in LHP}\right\} \qquad (26)$$

where LHP stands for left half plane. Under the assumption in (24), there are only first-order poles at $s = -v_{2n}$. The exact average PEP is given by

$$\begin{aligned}P\left[(\mathbf{c}, \mathbf{P}_{\tilde{u}}) \to (\hat{\mathbf{c}}, \mathbf{P}_{\hat{u}})\right] &= \sum_{k=0}^{N-1} \frac{v_{1k}v_{2k}}{v_{2k}(v_{1k} + v_{2k})} \\ &\quad \times \prod_{\substack{n=0 \\ n \neq k}}^{N-1} \frac{v_{1n}v_{2n}}{(v_{1n} + v_{2k})(v_{2n} - v_{2k})}. \qquad (27)\end{aligned}$$

However, this exact average PEP does not immediately give any insight. It is suitable for numerical computation only. We therefore device an approximation valid at high SNRs. From (22), for high SNR, we find that

$$\begin{aligned}&v_{1n} \simeq 0 \text{ and} \\ &v_{2n} \simeq \frac{\gamma_s(\gamma_e - 1)}{(\gamma_s + \gamma_e - 1)} = \Delta, \\ &\qquad n = 0, 1, \ldots, N-1. \qquad (28)\end{aligned}$$

Using (28) in the denominator of (24) and using (26), we have

$$\begin{aligned}&P\left[(\mathbf{c}, \mathbf{P}_{\tilde{u}}) \to (\hat{\mathbf{c}}, \mathbf{P}_{\hat{u}})\right] \\ &\qquad \simeq \mathrm{Res}\left\{\frac{G}{(-s)^{N+1}(s + \Delta)^N} \text{ at } s = -\Delta\right\} \qquad (29)\end{aligned}$$

where G is defined by (30), shown at the bottom of the page.

$$\begin{aligned}G &= \prod_{n=0}^{N-1} \frac{1}{4\left(\mu_{xx}\mu_{yy} - |\mu_{xy}|^2\right)} \\ &= \prod_{n=0}^{N-1} \left\{\frac{1}{\left(\frac{1}{\gamma_s} + \frac{1}{(\gamma_e - 1)} + \left|c_n e^{j\phi_n^{\tilde{u}}} - \hat{c}_n e^{j\phi_n^{\hat{u}}}\right|^2\right)\left(\frac{1}{\gamma_s} + \frac{1}{(\gamma_e - 1)}\right) - \left|\frac{1}{\gamma_s} + \frac{1}{\gamma_e}\hat{c}_n c_n^* e^{j(\phi_n^{\hat{u}} - \phi_n^{\tilde{u}})}\right|^2}\right\} \qquad (30)\end{aligned}$$

The Nth-order residue is evaluated as

$$\begin{aligned}
&\mathrm{Res}\left\{-\frac{1}{s^{N+1}(s+\Delta)^N} \text{ at } s=-\Delta\right\} \\
&\quad= \frac{(-1)^{N+1}}{(N-1)!}\frac{d^{N-1}}{ds^{N-1}}\left(\frac{1}{(-s)^{N+1}}\right)\Big|_{s=-\Delta} \\
&\quad= \frac{1}{(N-1)!}\frac{(N+1)(N+2)\ldots(2N-1)}{(-\Delta)^{2N}} \\
&\quad= \binom{2N-1}{N}\frac{1}{(\Delta^2)^N}. \qquad (31)
\end{aligned}$$

Combining (29) and (31), we finally get

$$P\left[(\mathbf{c},\mathbf{P}_{\tilde{u}})\rightarrow(\hat{\mathbf{c}},\mathbf{P}_{\hat{u}})\right] \simeq \binom{2N-1}{N} G\left(\frac{\gamma_s+\gamma_e-1}{\gamma_s(\gamma_e-1)}\right)^{2N}. \qquad (32)$$

Upon combining (30) and (32), we get (13).

ACKNOWLEDGMENT

The authors would like to thank the anonymous reviewers for their critical comments, which greatly improved this paper.

REFERENCES

[1] R. Nee and R. Prasad, *OFDM for Wireless Multimedia Communications*. Boston, MA: Artech House, Mar. 2000.

[2] E. A. Jones, T. Wilkinson, and S. Barton, "Block coding scheme for reduction of peak-to-mean envelope power ratio of multicarrier transmission schemes," *IEE Electron. Lett.*, vol. 30, no. 25, pp. 2098–2099, Dec. 1994.

[3] H. Ochiai and H. Imai, "Performance of the deliberate clipping with adaptive symbol selection for strictly band-limited OFDM systems," *IEEE J. Sel. Areas Commun.*, vol. 18, no. 11, pp. 2270–2277, Nov. 2000.

[4] K. G. Paterson and V. Tarokh, "On the existence and construction of good codes with low peak-to-average power ratio," *IEEE Trans. Inf. Theory*, vol. 46, no. 6, pp. 1974–1987, Sep. 2000.

[5] J. Tellado, "Peak to average power reduction for multicarrier modulation," Ph.D. dissertation, Dept. Elect. Eng., Stanford Univ., Stanford, CA, Sep. 1999.

[6] W. Henkel and V. Zrno, "PAR reduction revisited: An extension to Tellado's method," in *6th Int. OFDM Workshop*, Hamburg, Germany, 2001, pp. 31-1–31-6.

[7] A. D. S. Jayalath and C. Tellambura, "Use of data permutation to reduce the peak-to-average power ratio of an OFDM signal," *Wireless Commun. Mob. Comput. J.*, vol. 2, no. 2, pp. 187–203, Mar. 2002.

[8] S. H. Müller and J. B. Huber, "A comparison of peak power reduction schemes for OFDM," in *IEEE Global Telecommunications (GLOBECOM)*, Phoenix, AZ, 1997, vol. 1, pp. 1–5.

[9] M. Breiling, S. Müller-Weinfurtner, and J. Huber, "SLM peak–power reduction without explicit side information," *IEEE Commun. Lett.*, vol. 5, no. 6, pp. 239–241, 2001.

[10] Y. Xin and I. J. Fair, "Interpretation of coding for peak-to-average power ratio reduction in OFDM as constrained sequence coding and the application of guided scrambling," in *IEEE Int. Symp. Advances Wireless Communications*, Victoria, BC, Canada, 2002, pp. 121–122.

[11] N. Carson and T. A. Gulliver, "PAPR reduction of OFDM using selected mapping, modified RA codes and clipping," in *IEEE Vehicular Technology Conf.*, Vancouver, BC, Canada, 2002, pp. 1070–1073.

[12] K. Yang and S. I. Chang, "Peak-to-average power control in OFDM using standard arrays of linear block codes," *IEEE Commun. Lett.*, vol. 7, no. 4, pp. 174–176, Apr. 2003.

[13] A. D. S. Jayalath and C. Tellambura, "Blind SLM receiver for PAR reduced OFDM," in *IEEE Vehicular Technology Conf.*, Vancouver, BC, Canada, 2002, pp. 219–222.

[14] S. H. Müller and J. B. Huber, "A comparison of peak power reduction schemes for OFDM," in *IEEE Global Telecommunications (GLOBECOM)*, Phoenix, AZ, Nov. 1997, vol. 1, pp. 1–5.

[15] A. D. S. Jayalath and C. Tellambura, "A blind detection algorithm for PTS," in *IEEE Int. Symp. Advances Wireless Communications*, Victoria, BC, Canada, 2002, pp. 125–126.

[16] ——, "An adaptive PTS approach for the reduction of peak-to-average power ratio of an OFDM signal," *IEE Electron. Lett.*, vol. 36, no. 14, pp. 1161–1163, Jul. 2000.

[17] H. Ochiai, M. P. C. Fossorier, and H. Imai, "Performance analysis of deliberately clipped OFDM signals," *IEEE Trans. Commun.*, vol. 50, no. 1, pp. 89–102, Jan. 2002.

[18] J. Cavers and P. Ho, "Analysis of the error performance of trellis-coded modulations in Rayleigh-fading channels," *IEEE Trans. Commun.*, vol. 40, no. 1, pp. 74–83, Jan. 1992.

[19] C. Tellambura, "Evaluation of the exact union bound for trellis-coded modulations over fading channels," *IEEE Trans. Commun.*, vol. 44, no. 12, pp. 1693–1699, Dec. 1996.

[20] J. G. Proakis, *Digital Communications*, McGraw-Hill series in electrical engineering. Communications and signal processing, 4th ed. New York: McGraw-Hill, 2001.

[21] C. Tellambura and V. K. Bhargava, "Error performance of MPSK trellis-coded modulation over nonindependent Rician fading channels," *IEEE Trans. Veh. Technol.*, vol. 47, no. 1, pp. 152–162, Feb. 1998.